LICENTIATE THESIS

Nonlinear dynamic analysis of vertical rotors with tilting pad journal bearings

Gudeta Berhanu Benti

Machine Design

LULEÅ
UNIVERSITY
OF TECHNOLOGY

Licentiate Thesis

Nonlinear dynamic analysis of vertical rotors with tilting pad journal bearings

Gudeta Berhanu Benti

Luleå University of Technology
Department of Engineering Sciences and Mathematics
Division of Product and Production Development
971 87 Luleå, Sweden

Luleå, February 2022

Supervisors:

Jan-Olov Aidanpää and Rolf Gustavsson

Printed by Luleå University of Technology, 2022

ISSN: 1402-1757
ISBN: 978-91-7790-946-0 (print)
ISBN: 978-91-7790-947-7 (electronic)

Luleå 2022

www.ltu.se

“The problem with linear theory is that it is not nonlinear” – John A. Adam

Preface

The research presented in this thesis has been carried out at the division of Machine Design, Department of Engineering Sciences and Mathematics, Luleå University of Technology, and as a part of "Swedish Hydropower Centre - SVC". SVC has been established by the Swedish Energy Agency, Energiforsk and Svenska Kraftnät together with Luleå University of Technology, KTH Royal Institute of Technology, Chalmers University of Technology, Uppsala University and Lund University.

Participating companies and industry associations are: Andritz Hydro, Boliden, Fortum Sweden, Holmen Energi, Jämtkraft, Karlstads Energi, LKAB, Mälarenergi, Norconsult, Rainpower, Skellefteå Kraft, Sollefteåforsen, Statkraft Sverige, Sweco Sverige, Tekniska verken i Linköping, Uniper, Vattenfall R&D, Vattenfall Vattenkraft, Voith Hydro, WSP Sverige, Zinkgruvan and AFRY.

I would like to express my gratitude to my supervisor Prof. Jan-Olov Aidanpää for tremendous support and guidance. We had many interesting discussions about rotordynamics during these years, and I appreciate for taking the time to share his knowledge and many years of experience. I would like to thank my co-supervisor Dr. Rolf Gustavsson, for his valuable assistance. I am very grateful for his insightful suggestions and comments on the research project. Many thanks to Sune Andersson for his contribution during experimentation in Vattenfall test facility, Älvkarleby.

I would like to thank my former and current colleagues at the Division of Machine Design for bringing their best to work and make the workplace more enjoyable. A special thanks to my office-mate David Rondon for interesting discussions about various topics related to rotordynamics and our projects. I would like to extend my sincere thanks to colleagues at the Division of Manufacturing Systems Engineering for our interesting Fika and lunch break chats.

Great thanks to my family for their support and encouragement and for always being there for me. Dad and Mom, you are always the best!

Finally, I thank God for this opportunity and for I was healthy during my research time.

Gudeta Berhanu Benti
Luleå, Sweden
February 2022

Abstract

Hydropower is one of the key renewable energy resources in the world. For many years, hydropower machines have undergone continuous improvements and have adapted new technologies to cope with the growing energy demand. These improvements include design modifications and operation optimizations to increase efficiency and promote environmental sustainability. Like any other rotating machine, the dynamics of hydropower units are highly influenced by the supporting devices. Optimal and reliable supports are crucial to avoid excessive vibration that can lead to machine breakdown. Hydrodynamic journal bearings provide radial support to rotating parts, and they are important in reducing vibrations as they introduce damping to the system. In vertical hydropower rotors, tilting pad journal bearings (TPJBs) are commonly preferred because of their excellent stability performance. In contrast, however, these bearings can cause self-induced vibrations, resulting in rotor-bearing instability. This thesis focused on vertical rotors supported by TPJBs. Two types of bearings were considered, four-pad and eight-pad TPJBs. The dynamics of such a rotor-support system were studied, and the bearings' contribution to the system's overall performance was investigated.

Furthermore, accurate and reliable simulation models are important to learn and understand the dynamics of such systems at any stage in the product development process. Unlike horizontal rotors, vertical rotors have no stationary operation point due to the dead weight of the rotor, and the bearing dynamics vary with the position of the shaft. This means that the fluid film lubrication model of the bearings has to be calculated at each time step, which requires high computational effort. The classical simulation methods can be heavy for machines operating under varying conditions and require impractically long computational time. In such cases, an efficient and fast numerical simulation method, which does not significantly affect the accuracy of the result, is required. This thesis presented a numerical simulation procedure by pre-calculating the bearing coefficients instead of computing the fluid film lubrication model at each time step. The dependency of the bearing coefficients on the rotor speed was taken into account. The stiffness and damping coefficients of the bearing were represented by 2D polynomial equations as a function of eccentricity and rotor speed. The unbalance response of the vertical rotor-support system was simulated, and the results were validated by experiments for both stationary and non-stationary operation conditions.

List of publications

The thesis is composed of the following three appended papers:

Paper A	**Numerical and experimental study on the dynamic bearing properties of a four-pad and eight-pad tilting pad journal bearings in a vertical rotor.** Gudeta Berhanu Benti, David Rondon, Rolf Gustavsson, Jan-Olov Aidanpää: published in Journal of Energy Resource Technology (2021)
Paper B	**Speed-dependent stiffness and damping characteristics of a four-pad tilting pad journal bearing in vertical rotors.** Gudeta Berhanu Benti, Jan-Olov Aidanpää, Rolf Gustavsson submitted to International Journal of Rotating Machinery (2021)
Paper C	**The start-up dynamics of a vertical rotor with four pad tilting pad journal bearing.** Gudeta Berhanu Benti, Jan-Olov Aidanpää, Rolf Gustavsson will be submitted to International Journal of Rotating Machinery (2021)

Other publication

Other scientific contribution that is not included in the thesis:

- **Rotordynamic Characterization of Tilting-Pad Bearings With Eight Pads in Vertical Rotors.** David Rondon, Gudeta Berhanu Benti, Jan-Olov Aidanpää, Rolf Gustavsson published in Journal of Energy Resource Technology (2021)

Nomenclature

Symbol	**Units**	**Descriptions**
C_{ij}^{max}	Ns/m	Maximum damping coefficient in the local $i,j \rightarrow \xi,\eta$ coordinate
C_{ij}^{min}	Ns/m	Minimum damping coefficient in the local $i,j \rightarrow \xi,\eta$ coordinate
$\mathbf{C_{\beta}}$	Ns/m	Bearing damping matrix in the local coordinate
$\mathbf{C_{B}}$	Ns/m	Bearing damping matrix in the stationary coordinate
d	m	Position of unbalance mass from the center of the bearing
e, e_1	m	Eccentricity, given eccentricity
$\mathbf{f_u}$	N	Unbalance forces
G	Kgm^2	Gyroscopic matrix
K_{ij}^{max}	N/m	Maximum stiffness coefficient in the local $i,j \rightarrow \xi,\eta$ coordinate
K_{ij}^{min}	N/m	Minimum stiffness coefficient in the local $i,j \rightarrow \xi,\eta$ coordinate
K_{ij}^{eqv}	N/m	Equivalent stiffness coefficient in the local $i,j \rightarrow \xi,\eta$ coordinate
$\mathbf{K_{\beta}}$	N/m	Bearing stiffness matrix in the local coordinate
$\mathbf{K_{B}}$	N/m	Bearing stiffness matrix in the stationary coordinate
$\mathbf{K_{S}}$	N/m	Bracket stiffness matrix in the stationary coordinate
m_u	Kg	Unbalance mass
M	kg	Mass matrix
T	-	Transformation matrix
α	rad	Load angle

Ω	Rad/s	Angular velocity of the rotor (for steady-state)
$\dot{\phi}$	Rad/s	Angular velocity of the rotor (for non-stationary process)
$\ddot{\phi}$	Rad/s^2	Angular acceleration of the rotor
ε	%	Eccentricity ratio

Abbreviations

LBP	Load between pad
LOP	Load on pad
TPJB	Tilting pad journal bearing
1D	One-dimensional
2D	Two-dimensional

Contents

Preface v
Abstract vii
List of publications ix
Other publication x
Nomenclature xi
Part I 1
1 Thesis Introduction 3
  1.1 Basic rotordynamics 3
  1.2 Hydropower system 4
  1.3 Research Objective 5
  1.4 Structure of the thesis 5
2 Modelling of vertical rotors with TPJBs 7
  2.1 Introduction 7
  2.2 Tilting pad journal bearing model 8
    2.2.1 1D fitting of the bearing coefficients 10
    2.2.2 2D fitting of the bearing coefficients 12
  2.3 A vertical rotor rig and numerical modelling 13
    2.3.1 Description of the rotor rig 13
    2.3.2 Steady-state response simulation 14
    2.3.3 Non-stationary response simulation 17
3 Scope of the papers 21
  3.1 Paper A 21
  3.2 Paper B 22
  3.3 Paper C 23
4 Conclusions and Future outlooks 25
  4.1 Key findings of the thesis 25
  4.2 General conclusions of the thesis 26
  4.3 Future outlooks 26
5 References 29
Part II 31
6 Paper A 33
7 Paper B 59
8 Paper C 91

Part I

CHAPTER 1

Thesis Introduction

1.1 Basic rotordynamics

Rotordynamics is a field in engineering that deals with the dynamics of rotating machines, such as compressors, turbines, and pumps. In general, such machines are composed of three main groups of components. These are the rotating components (rotor), the stationary components (foundation or supporting structure), and interconnections (bearings). The study of rotating machines covers several other disciplines, such as solid mechanics, fluid dynamics, or electromagnetism. Rotordynamics is essential, and the knowledge about the dynamics of such machines can save both economic losses and human fatality. One reason why it is necessary to study rotordynamics is to learn more about the dynamics of such machines at the earlier stage in the product development process. This knowledge is important and helps designers to choose appropriate components that are robust and reliable for their specific application. The rotating machines are exposed for vibrations during operation [1–4], which could be due to an unbalance mass, instabilities due to oil-whirl (oil-whip), and harmonic bearing excitation. It is, therefore, necessary to identify the potential sources of vibrations earlier in the design stage to come up with possible solutions and avoid or minimize harmful vibrations. On the other hand, rotordynamics is also an important tool in fault diagnostics and condition monitoring. It provides knowledge and helps the designers or operators decide whether it is safe to run the machine or take important measures to avoid failure.

1.2 Hydropower system

Hydropower unit converts mechanical energy into electricity as running water rotates the turbine and allows the generator to convert the potential energy of moving water into electricity. It is one of the key renewable sources of energy in the world. In 2020, more than 40% of the total energy consumption of Sweden comes from hydropower. Other energy resources include such as nuclear power and wind power, and the total annual supplied energy in Sweden from 1979 to 2019 is shown in Figure 1.

The majority of the hydropower units in Sweden are more than 50 years old and may require upgrading and refurbishment in recent years. The renovation measures include component replacement and different kinds of design modifications. The spinning mass (such as shaft or generator) of these machines is large, and a failure can cause catastrophes, leading to high economic losses. It is, therefore, important to have components that are robust, reliable, and easy to maintain. Besides, fast and accurate numerical simulation models are important to perform multiple simulations of different cases within a short computational time.

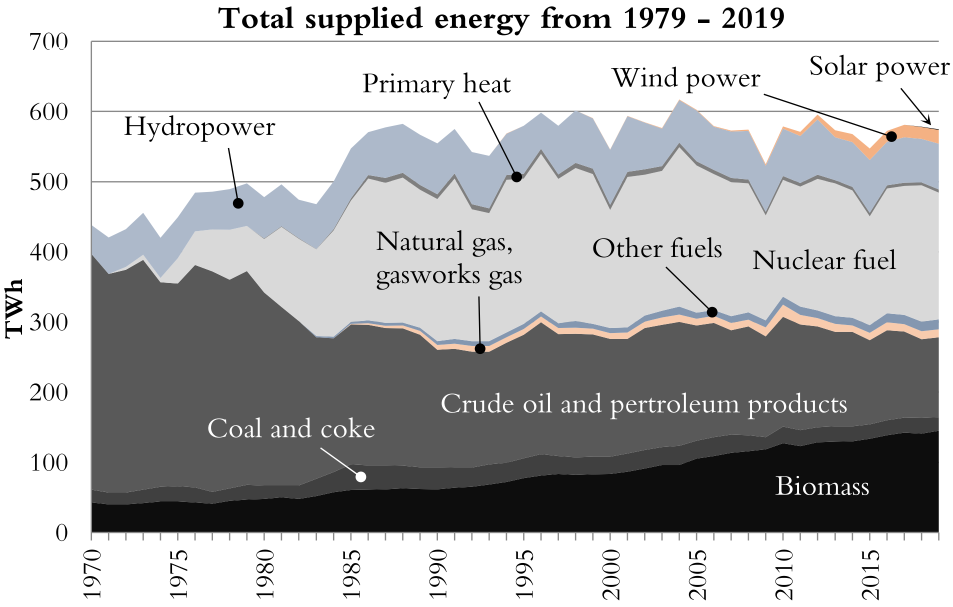

Figure 1: Total energy supply in Sweden. Source: Swedish Energy Agency [5] *and SCB* [6]. *Notes: 1) Other fuels are included in biomass prior to 1983. 2) International aviation included until 1989. 3) Nuclear fuel is reported gross, i.e. as supplied nuclear fuel energy, in accordance with UNECE guidelines. 4) Heat pumps in district heating plants. 5) Including wind power until 1989.*

1.3 Research Objective

In rotating machinery, bearings are known to be the primary sources of damping and have a significant influence on the dynamics of the rotor-bearing system. During the past 100 years, extensive research has been carried out on bearings used in different applications. Several modifications have been suggested and implemented to improve their static and dynamic properties. In rotordynamics, fluid film bearings are usually preferred over roller bearings because of their higher damping advantages and other characteristics. In contrast, there are some shortcomings with the fluid film bearings, such as hydrodynamic instability. This thesis focused mainly on the dynamics of vertical rotors with TPJBs and simulation models for steady-state and non-stationary processes. The main aims of this research are:

- to study and understand the dynamics of TPJBs in vertical rotor installations for a wide range of operations. Two types of bearings, i.e., four-pad and eight-pad TPJBs, were considered, and how these bearings could be a source of vibrations was investigated.
- to improve the efficiency of the numerical simulation models of vertical rotors with TPJBs in terms of computational time. The bearing coefficients of the four-pad TPJBs were pre-calculated and represented by 2D polynomial equations. Unbalance responses of the steady-state and non-stationary processes were simulated and validated by experiment.

1.4 Structure of the thesis

This licentiate thesis comprised of five chapters. Chapter 1 gives an introduction and overview of the rotordynamics and hydropower systems. Besides, the motivation and the main aims of the thesis are presented. Chapter 2 discusses the numerical simulation procedure of vertical rotors with TPJBs. The numerical and experimental results of steady-state and non-stationary operations are discussed. Chapter 3 presents the scope of the appended research papers. Chapter 4 discusses the overall thesis conclusion and future outlook. Chapter 6 contains references that are used in the thesis

CHAPTER 2

Modelling of vertical rotors with TPJBs

2.1 Introduction

This chapter is dedicated to presenting a nonlinear bearing model of TPJBs in vertical rotor installation. The dynamics of a vertical rotor rig, supported by two TPJBs, were studied both numerically and experimentally. In previous research [7], the bearing coefficients were pre-calculated and represented by 1D polynomial equations as a function of eccentricity. In this thesis, the model took into account the dependency of the bearing coefficients on the rotor speed. The bearing coefficients were represented by 2D polynomial equations with two independent variables; eccentricity and rotor speed. The computational efficiency of the model in terms of simulation time was investigated and compared with the classical simulation method that requires solutions from the fluid film lubrication model at each time step. The unbalance responses of the vertical rotor with TPJBs were simulated for steady-state and non-stationary processes. The simulation results were validated by those from the experiment.

The flowchart of the simulation procedure is shown in Figure 2.a. The simulation was carried out in two steps. In the first part of the simulation (Part I), the bearing coefficients were calculated by solving the Navier-Stokes equations for a number of cases. The calculated values were then fitted using curve- or surface-fitting techniques, and the bearing coefficients were represented by polynomial (exponential) equations. In the second part of the simulation procedure (Part II), the steady-state or the non-stationary response analyses were calculated by numerical integration procedures. The bearing model from Part I was used as an input to Part II. Moreover, the flow chart of the classical simulation procedure is shown in Figure 2.b. Unlike the model presented in this thesis (Model I), the classical simulation model (Model II) requires solutions from the fluid film lubrication model at each time step in the numerical integration procedure.

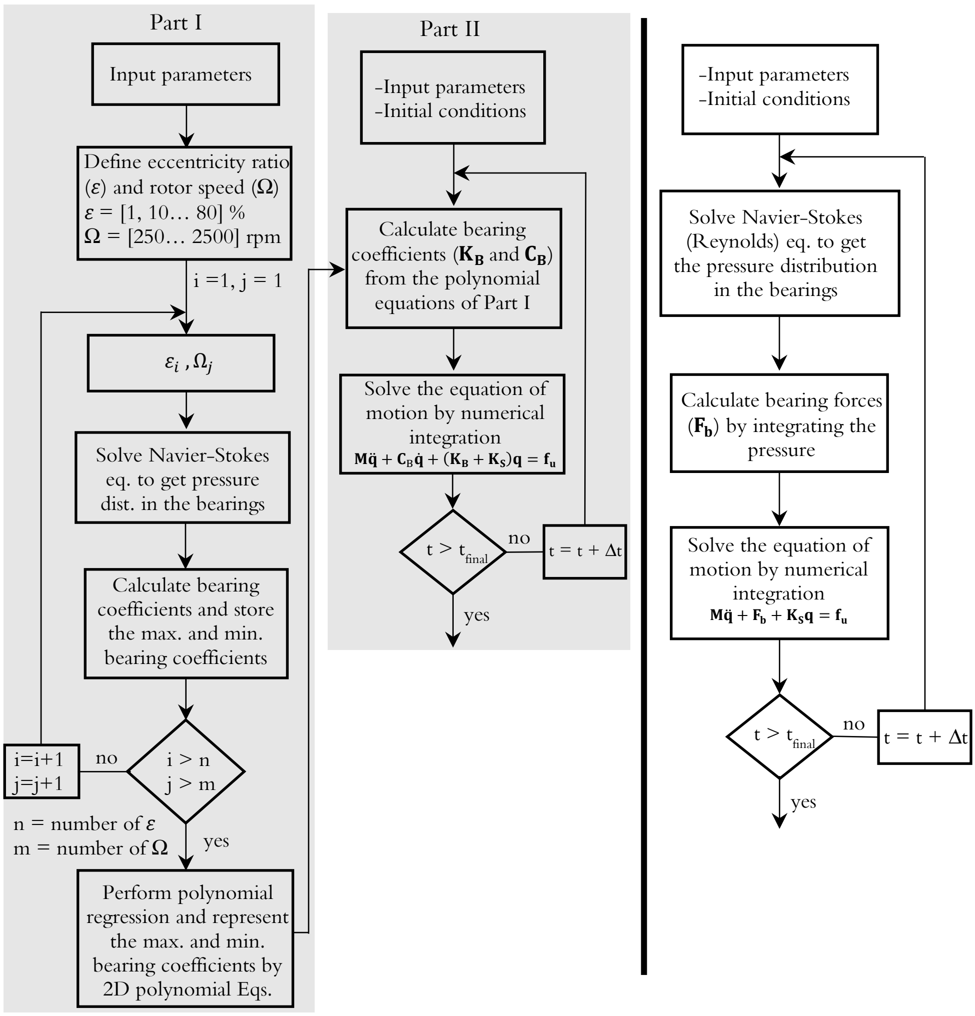
Part I
Input parameters
Define eccentricity ratio (ε) and rotor speed (Ω)
ε = [1, 10… 80] %
Ω = [250… 2500] rpm
i =1, j = 1
ε_i , Ω_j
Solve Navier-Stokes eq. to get pressure dist. in the bearings
Calculate bearing coefficients and store the max. and min. bearing coefficients
i > n
j > m
no
i=i+1
j=j+1
n = number of ε
m = number of Ω
yes
Perform polynomial regression and represent the max. and min. bearing coefficients by 2D polynomial Eqs.
Part II
-Input parameters
-Initial conditions
Calculate bearing coefficients ($\mathbf{K_B}$ and $\mathbf{C_B}$) from the polynomial equations of Part I
Solve the equation of motion by numerical integration
$\mathbf{M\ddot{q}} + \mathbf{C_B\dot{q}} + (\mathbf{K_B} + \mathbf{K_S})\mathbf{q} = \mathbf{f_u}$
$t > t_{final}$
no
$t = t + \Delta t$
yes
-Input parameters
-Initial conditions
Solve Navier-Stokes (Reynolds) eq. to get the pressure distribution in the bearings
Calculate bearing forces ($\mathbf{F_b}$) by integrating the pressure
Solve the equation of motion by numerical integration
$\mathbf{M\ddot{q}} + \mathbf{F_b} + \mathbf{K_S q} = \mathbf{f_u}$
$t > t_{final}$
no
$t = t + \Delta t$
yes

a) Model I *b) Model II*

Figure 2: The flowchart of the simulation procedure a) the model presented in the thesis b) the classical simulation model.

2.2 Tilting pad journal bearing model

Bearings have a significant influence on the dynamics of the rotating machines. Unlike vertical rotors, horizontal rotors usually have a stationary operation point due to a static load. In contrast, the performance of the bearings in vertical rotors is continuously changing since such machines have no stationary operation point. The numerical simulations for the dynamic response of such machines are expensive in terms of simulation time as the bearing forces have to be calculated by solving the fluid film lubrication model for each discrete time step. To reduce this computational effort, Näselqvist et al. [7] pre-calculated the stiffness and damping coefficients for different cases and represented them by 1D polynomial equations.

Figure 3 shows the schematic representation of the four-pad and eight-pad TPJBs with a 60% pivot offset. The geometry and operation parameters of the two bearing types are similar apart from their difference in the number of pads. The performance of the bearings varies depending on the position of the journal [8]. The local stiffness ($K_{\xi\xi}$) and damping ($C_{\xi\xi}$) coefficients are larger when the load is acting on-pads (LOP) compared to the load acting between-pads (LBP). Figure 4 shows the local stiffness coefficient ($K_{\xi\xi}$) changing periodically over the circumferential length of the four-pad TPJB.

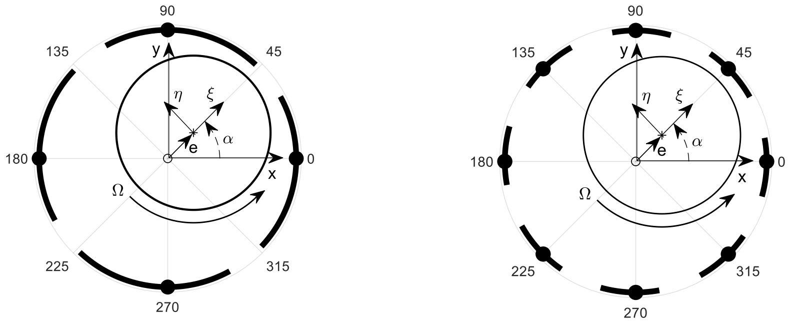

a) b)

Figure 3: A schematic representation of a) four-pad TPJB b) eight-pad TPJB.

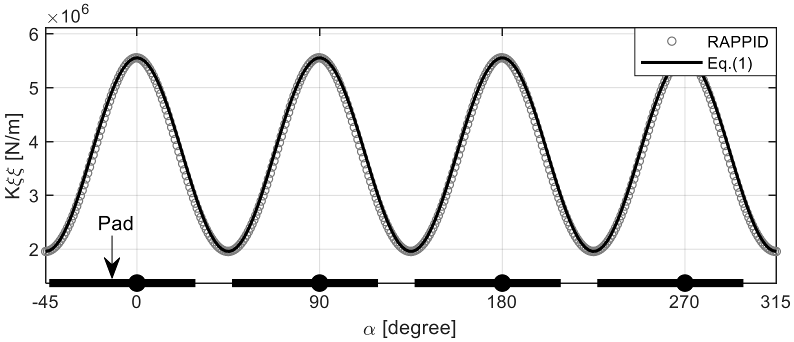

Figure 4: The local bearing stiffness ($K_{\xi\xi}$) at 1500rpm rotor speed and 60% eccentricity ratio.

The performances of the bearings, therefore, can be represented mathematically by sine and cosine functions. Once the maximum and minimum values are known, the bearing coefficients can be calculated for the entire circumferential locations using Eq. (1) and Eq. (2).

$$K_{ij}(\alpha,e) = \frac{K_{ij}^{max}+K_{ij}^{min}}{2}\ sign\ \frac{K_{ij}^{max}-K_{ij}^{min}}{2}\cdot\gamma \tag{1}$$

$$C_{ij}(\alpha,e) = \frac{C_{ij}^{max}+C_{ij}^{min}}{2}\ sign\ \frac{C_{ij}^{max}-C_{ij}^{min}}{2}\cdot\gamma \tag{2}$$

where

$$sign = \begin{cases} + & ij = \xi\xi \\ - & otherwise \end{cases}$$

$$\gamma = \begin{cases} cos\ (n\alpha) & i = j \\ \sin\ (n\alpha) & i \neq j \end{cases}, \qquad n{:}\, number\ of\ pads$$

2.2.1 1D fitting of the bearing coefficients

Maximum and minimum bearing coefficients: To calculate the bearing coefficients using Eq. (1) and Eq. (2), the maximum and minimum values have to be known. A commercial software package RAPPID [9] was used to solve the Navier-Stokes equations and calculate the maximum and minimum bearing coefficients as shown in Part I of Figure 2.a. The bearing coefficients were calculated for a single rotor speed, and the maximum and minimum bearing coefficients were represented using 1D polynomial (exponential) equations as a function of eccentricity ratio. Figures 5.a and 6.a show the local bearing stiffness of the four-pad and eight-pad TPJBs over a single pad, respectively. The maximum and minimum bearing coefficients of the two bearing types were calculated for different eccentricities. The values were fitted by an exponential function using MATLAB software, as shown in Figures 5.b and 6.b.

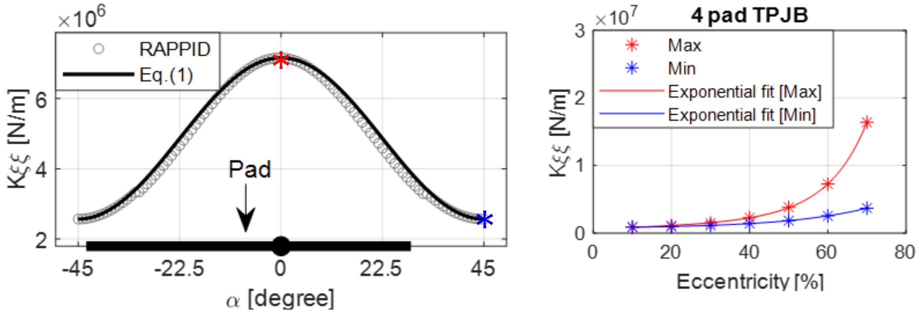

a) b)

Figure 5: a) Stiffness ($K_{\xi\xi}$) of the four-pad TPJB as a function of load angle. b) The maximum and minimum values are fitted using 1D exponential equations in MATLAB (exp2).

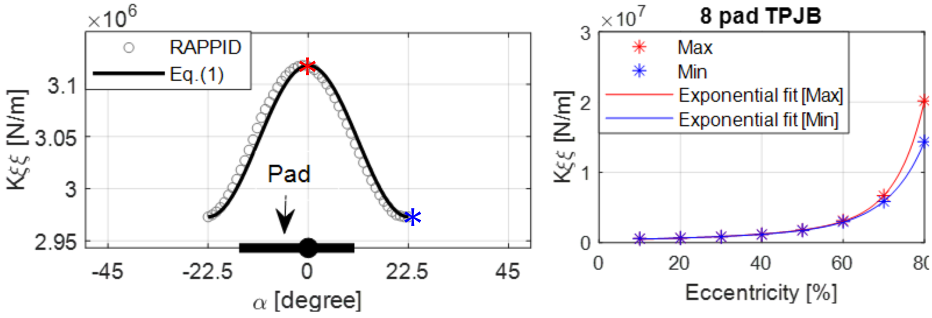

a) b)

Figure 6: Stiffness ($K_{\xi\xi}$) of the eight-pad TPJB as a function of load angle. b) The maximum and minimum values are fitted using 1D exponential equations in MATLAB (exp2).

Equivalent bearing stiffness coefficients: As shown in Figures 5.b and 6.b, the bearing coefficients are nonlinear, and the stiffness cannot be directly read from the stiffness-eccentricity curves. An equivalent stiffness coefficient, K_{ij}^{eqv}, which is the ratio of force (F_{ij}) to a given eccentricity (e_1), has to be calculated according to Eq. (3). Generally, the bearing force is the area under the stiffness-eccentricity curve and is calculated by integrating the stiffness over the eccentricity. For linear bearings, the equivalent stiffness coefficient is equal to the values read directly from the stiffness-displacement curve at a specific eccentricity.

$$K_{ij}^{eqv}(\alpha, e_1) = \frac{F_{ij}}{e_1} = \frac{\int_0^{e_1} K_{ij}(\alpha, e)de}{e_1} \tag{3}$$

Transformation from local to stationary coordinates: The calculated bearing coefficients were given in the local ξ and η coordinates. To use them in the rotor rig models given in Eq. (8) and Eq. (10), they have to be transformed to the stationary coordinates using Eq. (4) and Eq. (5).

$$\mathbf{K_B} = \mathbf{T^T K_\beta T} \tag{4}$$

$$\mathbf{C_B} = \mathbf{T^T C_\beta T} \tag{5}$$

where

$$\mathbf{T} = \begin{bmatrix} \cos(\alpha) & \sin(\alpha) \\ -\sin(\alpha) & \cos(\alpha) \end{bmatrix} \tag{6}$$

2.2.2 2D fitting of the bearing coefficients

One disadvantage of using 1D bearing coefficient equations is that it applies only to a specific rotor speed. These equations have to be re-calculated when operating speed changes. To find a general bearing model applicable for various operations, the bearing model has to consider the effect of the rotor speed. The bearing coefficients were represented by 2D polynomial equations as a function of eccentricity ratio (ε) and rotor speed (Ω). Figure 7 shows the maximum and minimum direct stiffness coefficients of the four-pad TPJB in the local ξ direction. The stiffness and damping coefficients were simulated by solving the Navier-stokes equation for six different rotor speeds and nine different eccentricity ratios. The datasets were fitted using a linear least-square method [10] and represented by 2D polynomial equations as shown in Eq. (7).

$$\begin{aligned}\tilde{Y} = {} & \beta_{00} + \beta_{10}\cdot\varepsilon + \beta_{01}\cdot\Omega + \beta_{20}\cdot\varepsilon^2 + \beta_{11}\cdot\varepsilon\cdot\Omega + \beta_{02}\cdot\Omega^2 \\ & + \beta_{30}\cdot\varepsilon^3 + \beta_{21}\cdot\varepsilon^2\cdot\Omega + \beta_{12}\cdot\varepsilon\cdot\Omega^2 + \beta_{03}\cdot\Omega^3 + \beta_{40}\cdot\varepsilon^4 \\ & + \beta_{31}\cdot\varepsilon^3\cdot\Omega + \beta_{22}\cdot\varepsilon^2\cdot\Omega^2 + \beta_{13}\cdot\varepsilon\cdot\Omega^3 + \beta_{50}\cdot\varepsilon^5 \\ & + \beta_{41}\cdot\varepsilon^4\cdot\Omega + \beta_{32}\cdot\varepsilon^3\cdot\Omega^2 + \beta_{23}\cdot\varepsilon^2\cdot\Omega^3\end{aligned} \tag{7}$$

where $\tilde{Y}$ is the maximum or minimum stiffness or damping coefficients. They are given in the local ξ and η coordinates. The polynomial coefficients (β_{ij}) of each bearing coefficient are given in Appendix B of paper B. The eccentricity ratio (e_p) and the rotor speed (Ω) are given in % and rpm, respectively.

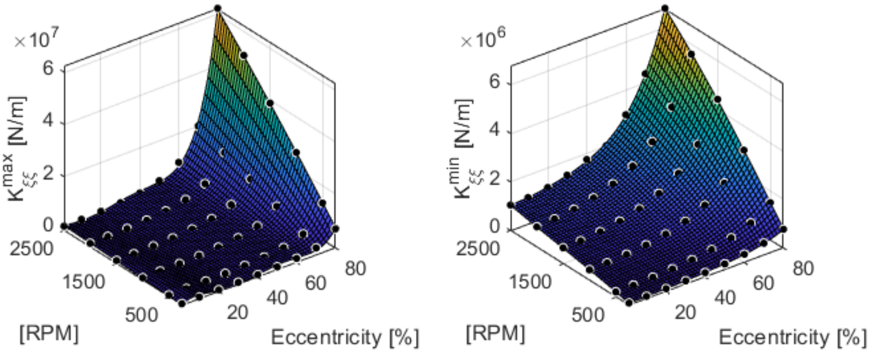

Figure 7: The maximum and minimum bearing stiffness ($K_{\xi\xi}$) of four-pad TPJB. The dataset, shown in black dots, is fitted with MATLAB function, poly53.

2.3 A vertical rotor rig and numerical modelling

2.3.1 Description of the rotor rig

Experimental tests were carried out on a test rig. The dimension of the rig is 1.1 m x 0.42 m x 0.42 m and oriented vertically [11]. It consisted of a mid-span rotor and two identical supports, as shown in Figure 8. The rotor was suspended vertically by a slender stinger, which was connected to an electric motor. The stinger is 4 mm in diameter and designed to support the rotor in the axial direction. In the radial direction, however, it is flexible and attached to two jaw couplings at the two ends of the stinger to minimize radial load transfer due to misalignment.

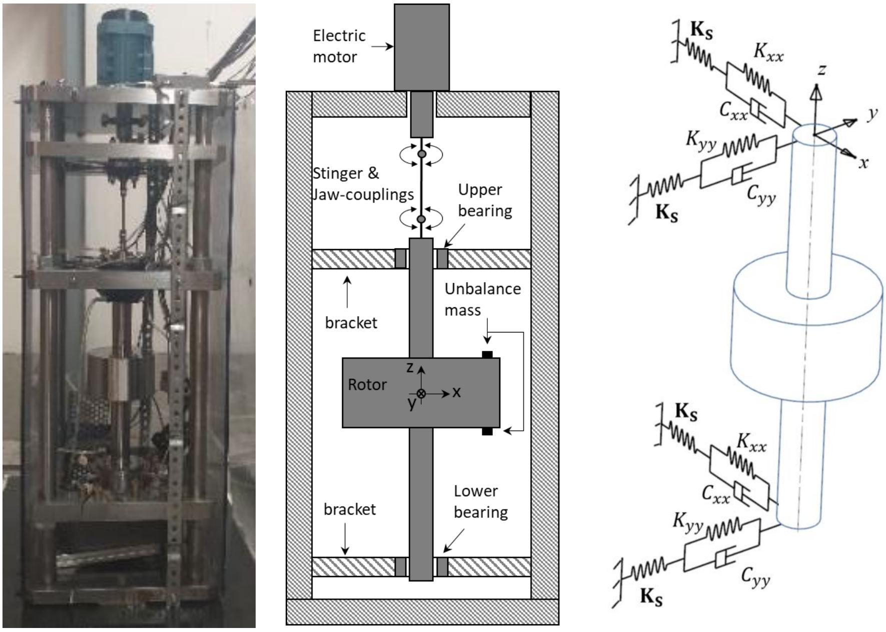
Electric motor
Stinger & Jaw-couplings
Upper bearing
Unbalance mass
bracket
Rotor
z
y
x
bracket
Lower bearing
$\mathbf{K_S}$
K_{xx}
C_{xx}
K_{yy}
C_{yy}
$\mathbf{K_S}$
z
y
x
$\mathbf{K_S}$
K_{xx}
C_{xx}
K_{yy}
C_{yy}
$\mathbf{K_S}$

a) b)

Figure 8: a) Rotor rig. b) A schematic representation of the rotor rig.

The support was composed of the four- or eight-pad TPJB and a bracket. The bracket is a flexible structure with a stiffness equal to 500MN/m and no damping [11]. The maximum operating speed of the electric motor is 3000rpm. The system was excited by an unbalance mass, mounted on the disk at a distance of 70mm from the disk's centre.

2.3.2 Steady-state response simulation

The steady-state response model of the rotor rig is represented mathematically, as shown in Eq. (8). The system has a total of eight degrees-of-freedoms (DOFs), $\mathbf{q} = [x_1 \ \ y_1 \ \ x_2 \ \ y_2 \ \ x \ \ y \ \ \theta \ \ \psi]^T$. The first four DOFs represent the translational displacements of the upper and lower brackets, whereas the last four DOFs denote the translational and rotational displacements of the rotor. The rotor was modelled as a rigid rotor since its first natural frequency is outside the frequency range of interest [12]. The vertically oriented rotor was supported by two flexible supports at the bottom and top end of the rotor. Each support consisted of the TPJB and bracket arranged in series. The equation of motion was reformulated in state-space form and solved numerically.

$$\mathbf{M}\ddot{\mathbf{q}} + (\Omega\mathbf{G} + \mathbf{C_B})\dot{\mathbf{q}} + (\mathbf{K_B} + \mathbf{K_S})\mathbf{q} = \mathbf{f_u} \tag{8}$$

where $\mathbf{M}$ is the mass matrix, $\mathbf{G}$ is the gyroscopic matrix, $\mathbf{C_B}$ is the damping matrix, $\mathbf{K_B}$ is the bearing stiffness matrix, $\mathbf{K_S}$ is the bracket stiffness matrix. The unbalance force vector ($\mathbf{f_u}$) is a nonlinear time-dependent function and is given as a function of unbalance magnitude ($m_u d$) and rotor speed (Ω).

$$\mathbf{f_u} = m_u d\Omega^2 \cdot \begin{bmatrix} 0 \\ 0 \\ 0 \\ 0 \\ cos(\Omega t) \\ sin(\Omega t) \\ 0 \\ 0 \end{bmatrix} \tag{9}$$

Key findings: The unbalance response of the vertical rotor supported by two identical TPJBs and brackets was investigated. The bearing coefficients were represented by 1D exponential equations. The displacement of the shaft and the force acting on the bearings are shown in Figure 9. The bearing dynamics periodically changed over the bearings' circumferential displacement, resulting in orbits with peaks and valleys. The orbits of the unbalance responses of the vertical rotor with two four-pad TPJBs were square-shaped, which is associated with the number of pads (n = 4). Large displacements were achieved when the load was located between pads (LBP), and the forces acting on the bearings were relatively larger at load on pads (LOP). Similarly, the bearing forces of the vertical rotor with eight-pad TPJBs were octagonal-shaped, due to the number of pads (n = 8). However, the displacement orbits were more circular-shaped since the difference between bearing coefficients at LOP and LBP was relatively small.

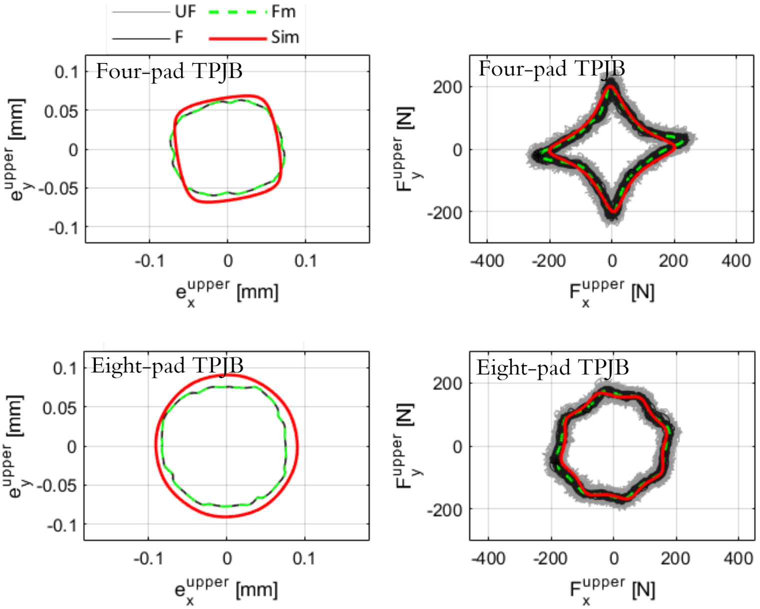

Figure 9: Displacement and force orbits of the four and eight-pad TPJB at 2000rpm and 5.9 x 10^{-3} Kgm unbalance magnitude. (UF=unfiltered measurement, F=filtered measurement, Fm= mean value of the filtered measurement, Sim=simulation)

The Fast Fourier Transform (FFT) of the steady-state unbalance responses for six different rotor speeds were calculated. Similarly, the bearing coefficients were pre-calculated and represented by 1D exponential equations. The exponential equations had to be re-calculated for each rotor speed. As shown in Figure 10, the simulation and experimental results show a similar trend. The first frequency order is due to the unbalance mass and is the dominating frequency order for both four-pad and eight-pad TPJBs. Besides, the four-pad TPJB is the source of vibrations at the 3rd and 5th frequency orders in the stationary coordinates, which are due to the number of pads (n±1, n: number of pads). In rotating coordinates, these frequency amplitudes appear as a single amplitude at the 4th frequency order.

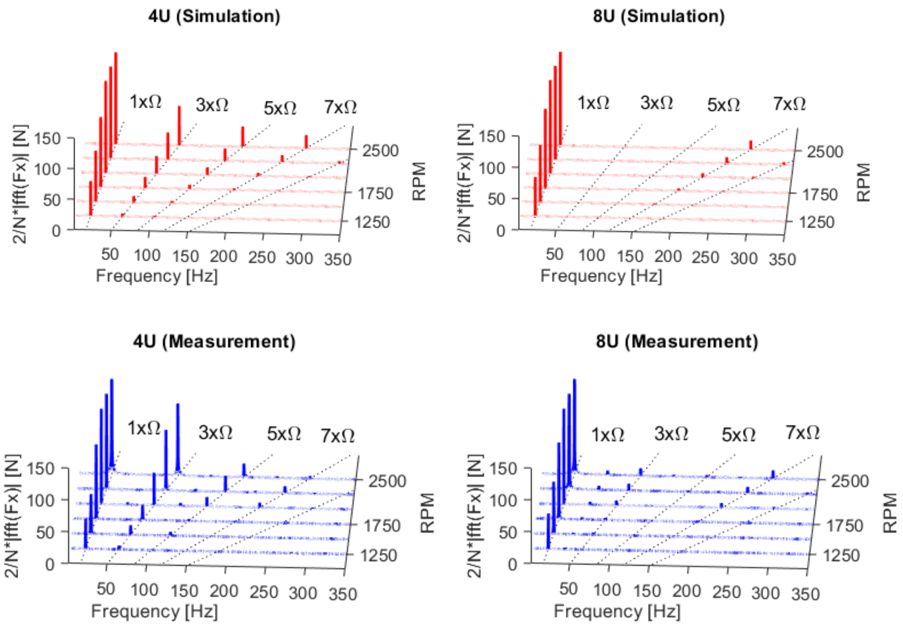

Figure 10: FFT of the measured bearing force of the four-pad and eight-pad TPJBs. The measured force of the upper four-pad TPJB (4U), lower four-pad TPJB (4L), upper eight-pad TPJB (8U) and lower eight-pad TPJB (8L) are considered. N is the number of samples

Moreover, the bearing coefficients were represented by the 2D polynomial equations (Eq. 7), and the steady-state unbalance responses of the vertical rotor with four-pad TPJBs were investigated under different unbalance magnitudes and rotor speeds. Like in the steady-state response simulations with 1D bearing exponential equations, the simulation results agreed with those in the experiments regarding the shape and magnitudes of the orbits. Furthermore, the computational efficiency of the simulation model was compared with the classical simulation procedure (Model II in Figure 2.b), which calculated the bearing forces by numerically solving the Reynolds equation at each time step [13–15]. The fluid domain was discretized into *MxN* number of elements, and a finite element model was employed to calculate the pressure distribution. For Model II, a plain-cylindrical journal bearing (ungrooved) was considered for simplification. The unbalance responses were calculated for 0.5 seconds when the rotor was running at 1500rpm and for an unbalance of $5.9 \cdot 10^{-3}$Kgm. The simulation was carried out on a standard laptop (Intel Core i7-8850H and CPU at 2.60 GHz) using MATLAB 2019a software. The computational time was obtained by *tic-toc* MATLAB command.

The simulation time required to perform the unbalance response of the vertical rotor with four-pad TPJB using Model I is 0.897 seconds. For Model-II, however, the computation time and accuracy depends on the number of elements used in the FEM. Figure 11 displays the response values and the computational time as a function of the number of elements in the bearing's circumferential direction (ϕ). A higher number of elements gives higher accuracy and larger computational time. Model I is effective in terms of computational time and it required at least three times less computational time compared to Model II. This ratio would have been larger if TPJBs were considered in Model II, instead of the plain-cylindrical journal bearing.

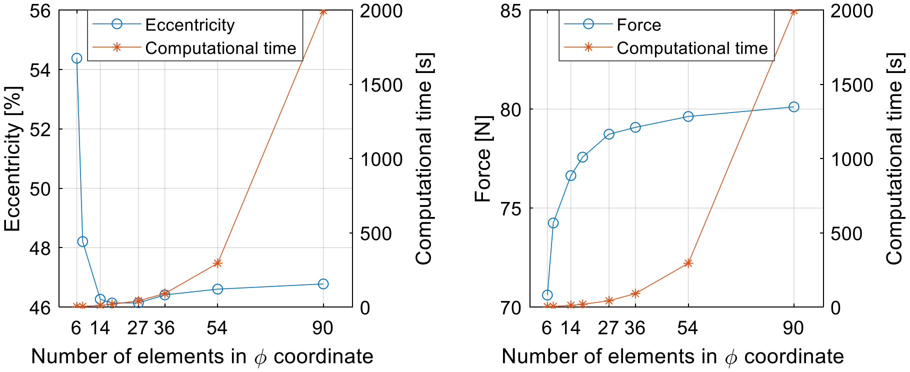

Figure 11: The computational time is plotted together with the eccentricity and force amplitudes as a function of number of elements in circumferential coordinate.

2.3.3 Non-stationary response simulation

For the non-stationary response simulation, the speed of the rotor increased linearly up to 2500rpm. The equation of motion was formulated as shown in Eq. (10). Unlike the steady-state response simulation, the non-stationary response equation contains extra terms due to the variable angular speed. Therefore, the left-hand side of Eq. (8) adds a matrix ($\ddot{\boldsymbol{\phi}}\boldsymbol{Gq}$) and affects the angular displacement terms of the two rotational DOFs. On the other hand, the right-hand side of the equation adds terms associated with the unbalance mass to the two rotor's translational DOFs; $m_u d\ddot{\phi}\, sin(\phi)$ and $-m_u d\ddot{\phi}\, cos(\phi)$.

$$\mathbf{M\ddot{q}} + \left(\dot{\phi}\mathbf{G} + \mathbf{C_B}\right)\mathbf{\dot{q}} + \left(\ddot{\phi}\mathbf{G} + \mathbf{K_B} + \mathbf{K_s}\right)\mathbf{q} \ = \mathbf{f_u} \tag{10}$$

where $\dot{\phi}$ is the angular speed, $\ddot{\phi}$ is the angular acceleration, which is the rate of change of the angular velocity ($\dot{\phi}$).

$$\mathbf{f_u} = \begin{bmatrix} 0 \\ 0 \\ 0 \\ 0 \\ m_u d\dot{\phi}^2 cos(\phi) + \ m_u d\ddot{\phi}\sin(\phi) \\ m_u d\dot{\phi}^2 sin(\phi) - m_u d\ddot{\phi}\cos(\phi) \\ 0 \\ 0 \end{bmatrix} \tag{11}$$

Key findings: The unbalance response of the vertical rotor with four-pad TPJBs for non-stationary conditions was investigated when the rotor speed was accelerated linearly from 250rpm to 2500rpm. The bearing coefficients were pre-calculated and represented by 2D polynomial equations. For both simulation and experimental results, the time series of the displacement and bearing forces were divided into 23 series intervals, and the maximum resultant responses were calculated at each interval. As shown in Figure 12, the unbalance responses increased with the rotor speed, and the simulation results agreed with those from the experiments. However, unlike simulation, an amplitude peak close to 1000rpm was observed in the experiments. It is due to the structural resonance of the test rig.

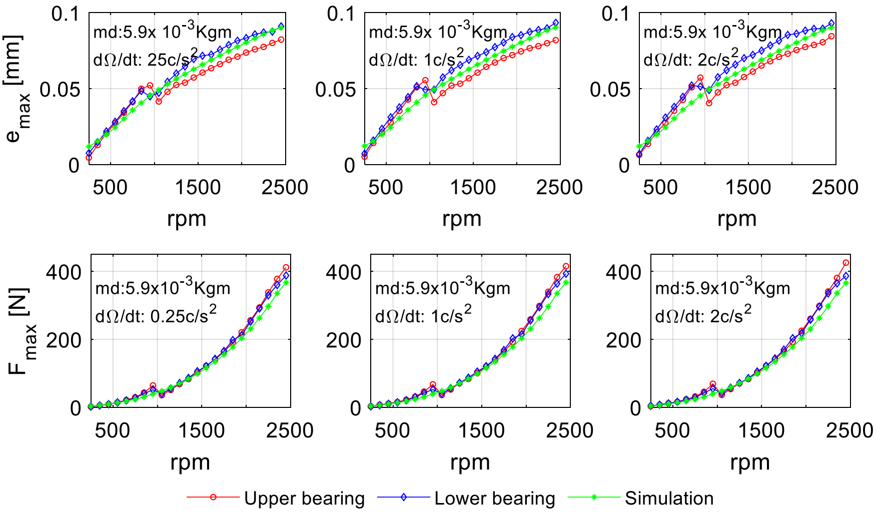

Figure 12: The simulated and measured displacements and bearing forces for 5.9 x 10^{-3}*Kgm and three angular accelerations.*

Furthermore, the FFT of the bearing forces in the stationary coordinates are displayed in the waterfall diagrams, Figures 13 and 14. The simulation results agreed with the results from the experiments. Both simulations and experiments showed that the first frequency order, which is due to the unbalance mass, was dominant. Like in steady-state response analysis, amplitudes peaks appeared at the 3rd and 5th frequency orders, which are due to the number of pads.

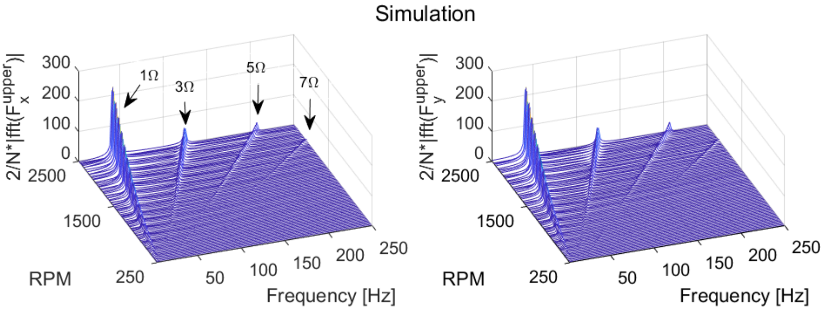

Figure 13: The waterfall diagrams of the simulated bearing forces for 5.9 x 10^{-3} Kgm and 1Cycle/s^2. N is the number of samples.

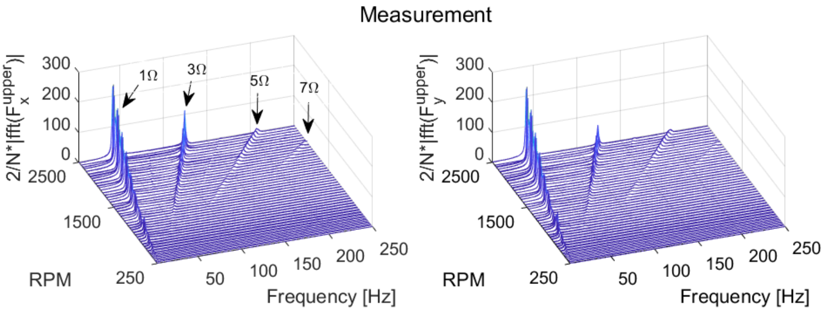

Figure 14: The waterfall diagrams of the measured bearing forces for 5.9 x 10^{-3}Kgm and 1Cycle/s^2. N is the number of samples.

CHAPTER 3

Scope of the papers

3.1 Paper A

Numerical and Experimental Study on the Dynamic Bearing Properties of a Four-Pad and Eight-Pad Tilting Pad Journal Bearings in a Vertical Rotor:

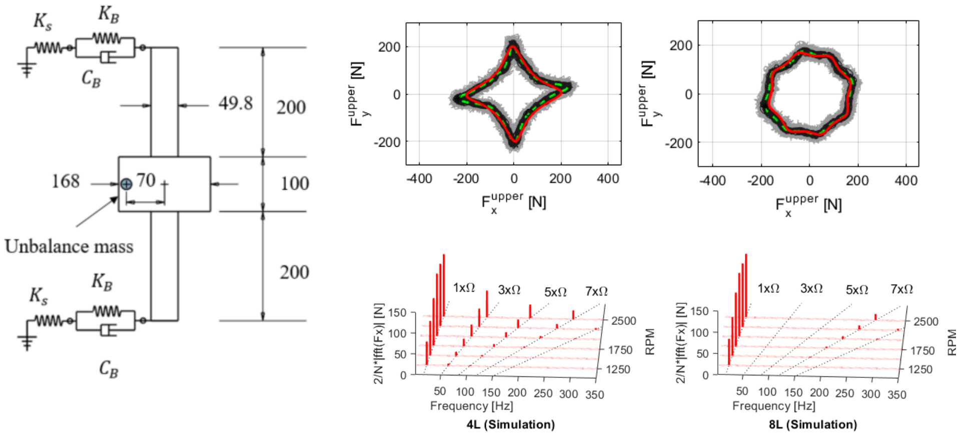

This paper investigated and compared the dynamics of the four-pad and eight-pad TPJBs in vertical rotor installation. The unbalance responses of the rigid vertical rotor supported by two identical TPJBs were simulated numerically and tested experimentally. The shape of the displacements and forces acting on the bearings were different for the two bearing types. Both numerical and experimental results showed that the TPJBs excited the rotor-support system and caused vibrations at frequencies associated with the number of pads. Unlike the eight-pad TPJB, the four-pad TPJB was the source of the 3Ω and 5Ω frequency orders in the stationary coordinates, and the amplitudes of these frequency orders increased with the rotor speed.

3.2 Paper B

Speed-dependent stiffness and damping characteristics of a four-pad tilting pad journal bearing in vertical rotors:

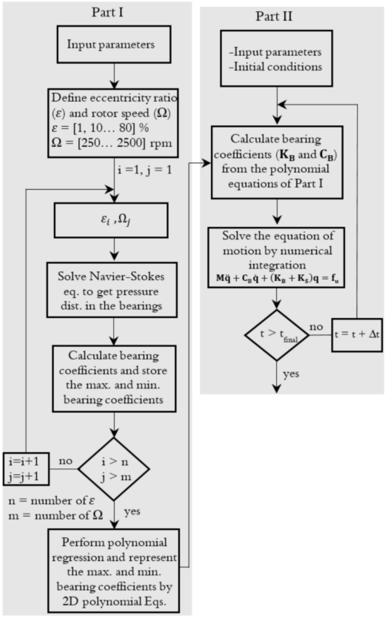
Part I
Input parameters
Define eccentricity ratio (ε) and rotor speed (Ω)
ε = [1, 10… 80] %
Ω = [250… 2500] rpm
i = 1, j = 1
ε_i, Ω_j
Solve Navier-Stokes eq. to get pressure dist. in the bearings
Calculate bearing coefficients and store the max. and min. bearing coefficients
i = i+1
j = j+1
no
i > n
j > m
yes
n = number of ε
m = number of Ω
Perform polynomial regression and represent the max. and min. bearing coefficients by 2D polynomial Eqs.
Part II
-Input parameters
-Initial conditions
Calculate bearing coefficients ($\mathbf{K_B}$ and $\mathbf{C_B}$) from the polynomial equations of Part I
Solve the equation of motion by numerical integration
$\mathbf{M\ddot{q}} + \mathbf{C_B\dot{q}} + (\mathbf{K_B} + \mathbf{K_s})\mathbf{q} = \mathbf{f_u}$
t > t$_{final}$
no
t = t + Δt
yes

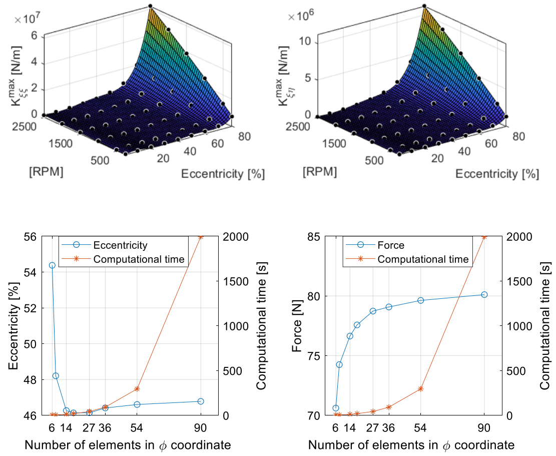

The paper presented a simplified steady-state simulation model for vertical rotors with TPJBs. Adapting the classical simulation procedures to simulate such models requires solving the fluid film lubrication model at each time step, which is computationally expensive. A previous study attempted to reduce the computation time by describing the bearing coefficients using 1D polynomial equations instead of solving the fluid film lubrication model. One limitation of this model is that the polynomial equations apply only for one rotor speed and the bearing coefficients have to be recalculated if the rotor speed changes. In this paper, the bearing coefficients of a four-pad TPJB were represented by 2D polynomial equations. The steady-state unbalance response of the rotor rig was simulated numerically for a number of cases, and the results were validated by experiments. Compared to the classical model, the model presented in this paper was efficient in terms of computational time.

3.3 Paper C

The start-up dynamics of a vertical rotor with four-pad tilting pad journal bearing:

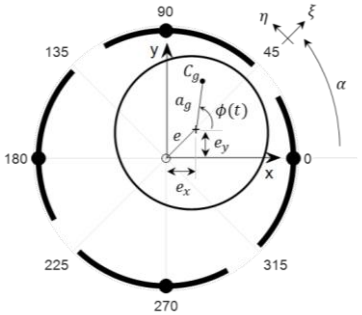

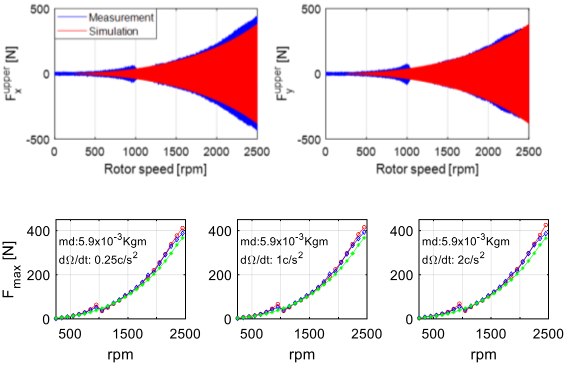

This paper is the continuation of Paper B and studies the dynamic response of a vertical rotor for non-stationary operation conditions. The bearing models developed in Paper B were used, and the non-stationary unbalance responses of the vertical rotor with two four-pad TPJBs were simulated for three different unbalance magnitudes. The rotor speed was increasing linearly from 250rpm to 2500rpm with three different angular acceleration rates. The simulation results agreed with the results from the measurements.

CHAPTER 4

Conclusions and Future outlooks

4.1 Key findings of the thesis

The key findings of the thesis is summarized as follows.

- The dynamics of the four-pad and eight-pad TPJBs in the vertical rotor was investigated and compared for a wide range of rotor speeds. The displacement and force orbits of the rotor with four-pad TPJBs were square-shaped, whereas the orbits of the rotor with eight-pad TPJBs were octagonal-shaped. This is because the bearing dynamics vary periodically over the circumferential displacement of the bearings. For the eight-pad TPJBs, however, the displacement orbits were circular-shaped as the difference in bearing coefficients at LOP and LBP were relatively smaller. Furthermore, unlike the rotor with eight-pad TPJBs, the four-pad TPJBs were the source of excitation at the third and fifth frequency orders in the stationary coordinates, which is due to the number of pads. The amplitudes of these frequency orders increased with the rotor speed.
- The steady-state and non-stationary unbalance response of the vertical rotor supported by two identical four-pad TPJBs was successfully modelled. The bearing coefficients of the four-pad TPJB were pre-calculated and represented by 2D polynomial equations. The simulated displacements and forces agreed with those from the experiments with some deviations. However, these deviations were expected as the bearing parameters used in the simulations were predicted values and could be different from the actual values. Besides, the measured displacement and bearing forces were affected by the structural resonance of the test rig at 1000rpm.
- The numerical simulation model by pre-calculating the bearing model is advantageous over the classical model in terms of computation time

4.2 General conclusions of the thesis

This thesis provides a scientific contribution in the area of rotordynamics, and the results from this research work are useful for researchers and designers of rotating machinery, particularly for vertical rotors with TPJBs. The steady-state and non-stationary response simulation models presented in Paper B and Paper C can be used to study and investigate the dynamics of such machines at different phases of the product development process. The simulation models are efficient in terms of computation time, as it does not require solving the fluid film lubrication model at each discrete time step.

Furthermore, this thesis provides numerical and experimental investigations on how the TPJBs could cause self-induced vibrations due to the number of pads. Running vertical rotors with TPJBs at a speed corresponding to the number of pads can potentially amplify vibrations and lead to resonance problems. Paper A presented numerical and experimental investigations on the dynamics of the four-pad and eight-pad TPJBs in vertical rotor installation. It has been observed that the four-pad TPJB is a source of vibration amplitudes at the 3Ω and 5Ω frequency orders in the stationary coordinates (or 4Ω in the rotating coordinates). Vibrations due to these frequency orders could potentially be avoided if the eight-pad TPJB or bearing with a larger number of pads are used.

4.3 Future outlooks

The potential future researches related to the presented work are highlighted as follows.

- In this thesis, the non-stationary dynamic analysis was performed on the rigid rotor, where the first natural frequency is outside the test frequency range. This made it impossible to study the dynamics of the rotor when passing through the critical speed. The study on the non-stationary dynamics of a flexible rotor, which its first natural frequency is within the test frequency range, is an interesting area of research.
- The simulation procedure developed in Paper B, which represented the coefficients of the four-pad TPJB by 2D polynomial equations, was validated using lab-based experiments. Future studies could be performed by considering different types of bearings to evaluate the generality of the method. Furthermore, the simulation procedure will also be used to simulate the dynamic response of real hydropower machines.
- In this thesis, the dynamics of the four-pad and eight-pad TPJBs were studied in a vertical rotor installation, and how they could potentially

cause self-induced vibrations due to the number of pads was discussed. Harmful vibrations, in general, in such machines could cause failure and have to be eliminate or minimized for smooth and safe operation. Further research is required to explore components that could potentially reduce such unfavourable vibrations in vertical machines.

REFERENCES

References

[1] Adams, M. l., and Payandeh, S., 1982, "Self-excited vibration of statically unloaded pads in tilting-pad journal bearings," J. Lubrication Technology, **105**, pp. 377–383, 1982

[2] Nishimura, .A, Inoue, T., and Watanabe, Y., 2018 "Nonlinear Analysis and Characteristic Variation of Self-Excited Vibration in the Vertical Rotor System Due to the Flexible Support of the Journal Bearing," J. Vibration and Acoustics, **140**(1), pp. 1–13, DOI: 10.1115/1.4037520

[3] Muszynska, A., 1986 "Whirl and whip-Rotor/bearing stability problems," J. Sound and Vibration, **110**(3), pp. 443-462. doi: 10.1016/S0022-460X(86)80146-8

[4] Synnegård, E., Gustavsson, R., and Aidanpää, J-O., 2016, "Forced response of a vertical rotor with tilting pad bearings," *Proc. 16th International Symposium on Transport Phenomena and Dynamics of Rotating Machinery*, Honolulu, United States.

[5] Swedish Energy Agency, https://www.energimyndigheten.se/en/.

[6] Statistiska centralbyrån, https://www.scb.se/.

[7] Nässelqvist, M., Gustavsson, R. and Aidanpää, J.O., 2014, "Experimental and Numerical Simulation of Unbalance Response in Vertical Test Rig with Tilting-Pad Bearings," International Journal of Rotating Machinery, **2014**(1), pp. 1 – 10. DOI: 10.1155/2014/309767

[8] Childs, D.W. and Carter, C.R., 2009, "Rotordynamic Characteristics of a 5 Pad, Rocker-Pivot, Tilting Pad Bearing in a Load-on-Pad Configuration: Comparisons to Predictions and Load-Between-Pad Results," *Proc. Of ASME Turbo Expo: Power for Land, Sea, and Air*, Florida, USA.

[9] Rotordynamic seal research, http://www.rda.guru/

[10] Lin, J. G., 2006, “Modeling test responses by multivariable polynomials of higher degrrees,” SIAM Journal on Scientific Computing, **28**(3), pp. 832–867.

[11] Nässelqvist, M., Gustavsson, R., and Aidanpää, J.-O., 2012, “Design of test rig for rotordynamic simulations of vertical machines,” Proc. of the 14th International Symposium on TransportPhenomena and Dynamics of Rotating Machinery, Honolulu, USA.

[12] Synnegård, E., Gustavsson, R., and Aidanpää, J. O., 2016, “Influence of Cross-Coupling Stiffness in Tilting Pad Journal Bearings for Vertical Machines,” International Journal of Mechanical Sciences, **111–112**, pp. 43–54. DOI: 10.1016/j.ijmecsci.2016.03.017

[13] Booker, J. F., and Huebner, K. H., 1972 “Application of finite element methods to lubrication: An engineering approach,” Journal of Lubrication Technology, **94**(4), pp. 313–323, DOI: 10.1115/1.3451719.

[14] Allaire, P. E., Nicholas, J. C., and Gunter, E. J., 1977, “Systems of Finite Elements for Finite Bearings,” Journal of Lubrication Technology, **99**(2), pp. 187-194, DOI: 10.1115/1.3453016

[15] Qiu, Z. L., 1994, “A theoretical and experimental study on dynamic characteristics of journal bearings,” Ph.D. Dissertation, University of Wollongong, Wollongong, Australia.

[16] Lund, J. W., 1964, “Spring and Damping Coefficients for the Tilting-Pad Journal Bearing,” ASLE Transactions, **7**(4), pp. 342–352. DIO: 10.1080/05698196408972064

Department of Engineering Sciences and Mathematics
Division of Product and Production Development

ISSN 1402-1757
ISBN 978-91-7790-946-0
ISBN 978-91-7790-947-7

Luleå University of Technology 2021

FSC
www.fsc.org
MIX
Papper från ansvarsfulla källor
FSC® C010493

SVANENMÄRKET
Trycksak
3041 3042

Print: Lenanders Grafiska, 4567294

LULEÅ
UNIVERSITY
OF TECHNOLOGY